Radiation Physics and Chemistry 171 (2020) 108732

Contents lists available at ScienceDirect

Radiation Physics and Chemistry

journal homepage: www.elsevier.com/locate/radphyschem

Influence of gamma irradiation on the properties of PbS thin films

Syed Mansoor Ali[a,*], M.S. AlGarawi[a], S. Aldawood[a,**], S.A. Al Salman[a], S.S. AlGamdi[a]

[a] Department of Physics and Astronomy, College of Science, P.O. BOX 2455, King Saud University, Riyadh, 11451, Saudi Arabia

ARTICLE INFO

Keywords:
PbS thin films
Gamma irradiation
SILAR
Band gap
Impedance spectroscopy
Photoluminescence

ABSTRACT

Thin films of lead sulfide (PbS) were prepared on glass substrates using the successive ionic layer adsorption and reaction technique. To investigate the gamma-induced properties, the deposited thin films were sequentially exposed to ^{60}Co gamma rays at doses varying from 0 to 75 kGy. X-ray diffraction analysis of the pristine and irradiated samples showed that the crystallinity of the PbS thin films increased with the gamma dose. Field-emission scanning electron microscopy revealed that the PbS particle size increased with the gamma dose up to 25 kGy, and then decreased. Defect peaks at 805.54 and 833.89 nm were found in the photoluminescence spectra of the pristine samples that were annihilated owing to the gamma exposure. Impedance spectroscopy indicated that the radiation effect increased the grain resistance as the dose level was increased. The noticeable changes induced in the structural, optical, and electrical properties of the PbS thin films clearly introduce the possibility of using them in gamma dosimetry application.

1. Introduction

Lead sulfide (PbS) is an important IV-VI binary compound semiconductor that has received significant attention due to its narrow energy band gap of 0.41 eV (Meldrum et al., 1996), and a relatively large Bohr radius of approximately 18 nm (Torimoto et al., 2002). PbS provides high quantum confinement for electrons and holes. Therefore, it is an interesting material whose energy band gap can be tuned, giving rise to several nanostructures, and optical and electrical properties that are more diverse than those of the bulk material. Due to its unique properties, PbS has been used in various devices such as IR detectors, diode lasers, transistors, contact rectifiers, and in applications such as solar absorption and photo-resistance (Putley, 1967; Ballard et al., 1972; Nair et al., 1992; Hirata and Higashiyama, 1971; Kane et al., 1996; Kanazawa and Adachi, 1998; Joshi et al., 2004). PbS thin films can be prepared using different physical and chemical deposition techniques such as chemical bath deposition (Seghaier et al., 2006), electrodeposition (Maheswassharon et al., 1997), spin-coating deposition (Patel et al., 2014), low-pressure spray pyrolysis (Thangaraju and Kalainnan, 2000), atomic layer deposition (Hsu et al., 2013), microwave heating (Yonghong et al., 2004), and solid-vapor deposition (Obaid et al., 2012). Successive ionic layer adsorption and reaction (SILAR) is the most appropriate technique for the deposition of PbS thin films. SILAR has a number of advantages, such as thickness control, low temperature requirement, freedom in choosing the elemental composition, and non-requirement of a high-quality target. Furthermore, it is inexpensive, simple, and convenient for large-area deposition (Bickulova et al., 1995; Chatterjee et al., 1999; Chen et al., 1985; Chopra et al., 1983; Danko et al., 1991).

It is believed that gamma radiations have the ability to relocate the atoms of the host materials from their lattice. This phenomenon is accountable for initiating the deviations in the nanostructure. Changes produced by the irradiation depend on the dose of the radiation, nature of the host material, and the angle of interaction (Ivanov and Platov, 2004). Several reports were published regarding the influence of gamma irradiation on the properties of thin films such as gamma irradiation of In_2O_3 and Cu_2ZnSnS_4 thin films (Nefzi et al., 2017; Mehdi et al., 2018) for photovoltaic applications. In some cases, gamma irradiations improved some physical properties (Azmy et al., 2017; Sofiany et al., 2014; Shabir et al., 2015). To the best of our knowledge, no previous study has been published on PbS thin films regarding the modification of structural, optical, and electrical properties induced by gamma irradiation. The interaction of nanomaterials with gamma radiation can lead to the formation of structural defects in the form of deficiencies, clusters, and dislocations (Zhu, 1998). These defects are actually the energy levels within the energy band gap that can act as carrier-trapping or carrier-recombination centers associated with the energy (Atanassova et al., 2001).

The novelty of this present study is to deposit the PbS thin films using the SILAR SILAR technique. The main objective of this study is, to

* Corresponding author.
** Corresponding author.
E-mail addresses: symali@ksu.edu.sa (S.M. Ali), sdawood@ksu.edu.sa (S. Aldawood).

https://doi.org/10.1016/j.radphyschem.2020.108732
Received 2 May 2019; Received in revised form 14 January 2020; Accepted 23 January 2020
Available online 27 January 2020
0969-806X/

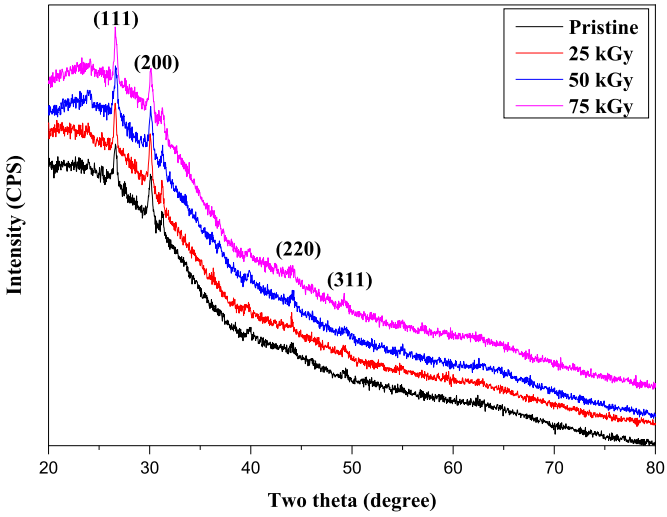

Fig. 1. XRD patterns for pristine and gamma-exposed PbS thin films.

tune the structural, optical, and electronic properties of PbS thin films that have been examined by varying the gamma irradiation dose. The gamma irradiation modified the crystallinity, particle size, surface morphology, energy band gap, photoluminescence, grain resistance, and grain capacitance of the PbS thin films.

2. Experimental

PbS thin films were deposited on the glass substrates using the SILAR technique. Before the deposition, the substrates were washed with dilute hydrochloric acid, methanol, and deionized water, and dried with nitrogen gas. For the thin film deposition, 0.5 M lead nitrate ($Pb(No_3)_2$; 99.999%) in water and 0.5 M sodium sulfide (Na_2S; > 99%) solution in ethanol were used as the cation (Pb^{2+}) and anion (S^{2-}) sources, respectively. First, the cleaned glass substrates were dipped in the cation solution for 30 s, rinsed with deionized water, and then dried at 100 ˚C for 2 min. Next, the same substrates were immersed in the anion solution for 30 s, rinsed with ethanol, and dried under the same temperature and time conditions. These two steps form one complete cycle of SILAR and leads to formation of PBS thin films. For homogeneity and sufficient thickness of the PbS thin films, 10 cycles were performed.

The deposited PbS thin films were irradiated with different gamma doses using a 1.25 MeV ^{60}Co source (half-life of 5.2714 years; Model SC220E, MDS Nordion), at dose rate of 7.328 kGy/h. The sample was placed perpendicularly at distance of 6.5 cm from the source. The samples were exposed to the radiation for 207, 415 and 622 min to acquire 25, 50, and 75 kGy gamma irradiation dose respectively.

The pristine and gamma-irradiated PbS thin films were structurally

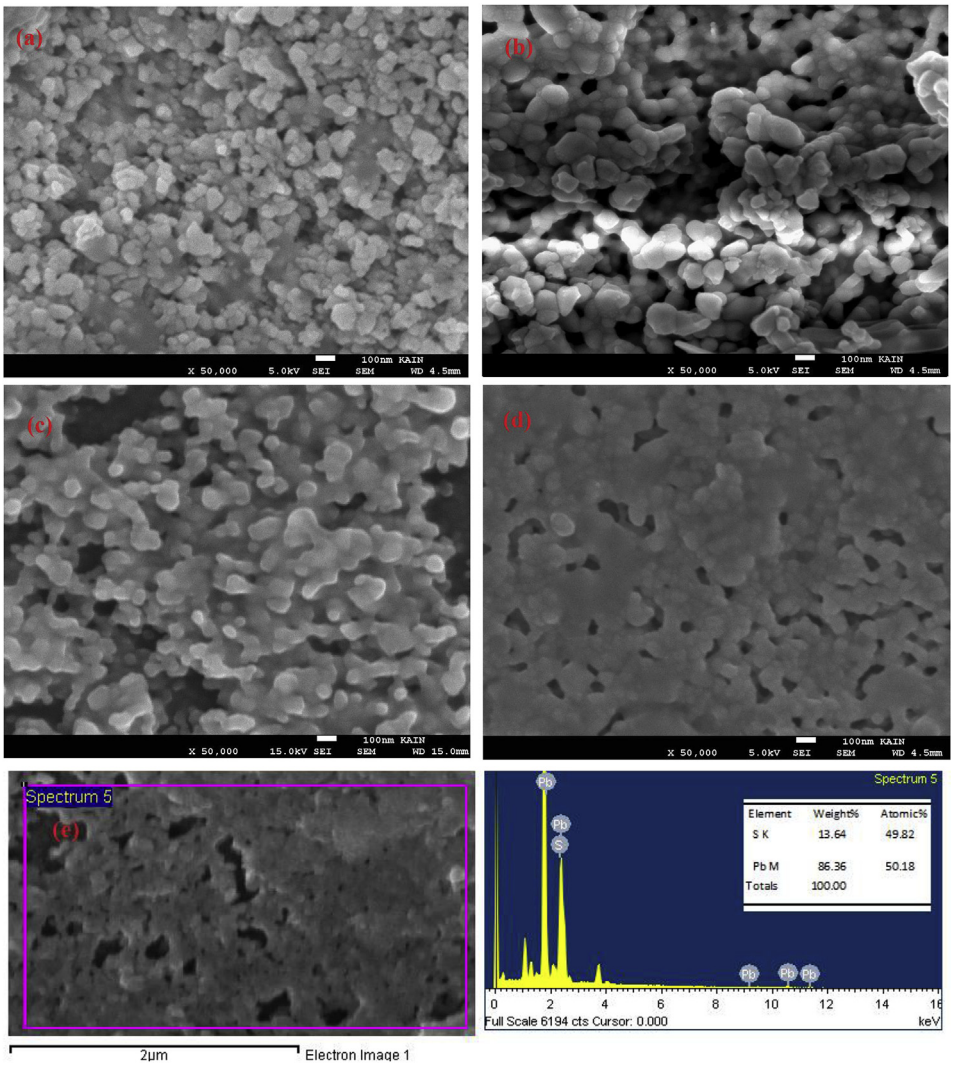

Figure 2. (a–d) FESEM images of PbS pristine thin film, and films exposed to 25, 50, and 75 kGy gamma doses, respectively, and (e) EDS spectrum of PbS thin film.

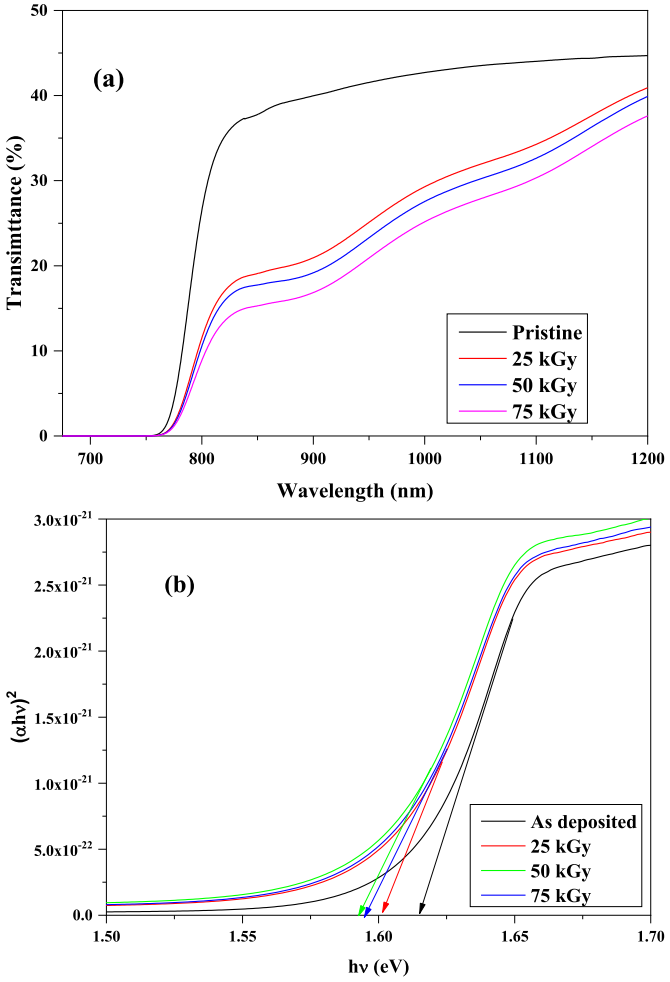

Fig. 3. (a) Transmission spectra and (b) Tauc plot of pristine and gamma exposed PbS thin films.

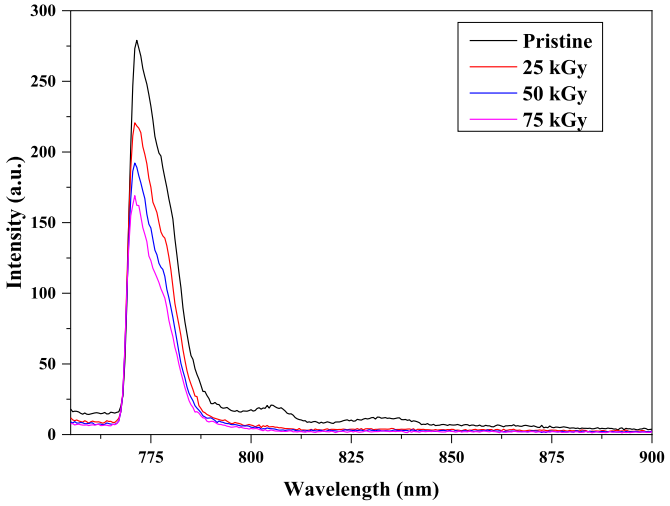

Fig. 4. PL spectra of pristine and gamma-exposed PbS thin films.

examined using an X-ray diffractometer (PANalytical X'Pert^3 MRD X) with a CuKα radiation source. The morphology of the thin films was studied using a scanning electron microscope (JEOL). The optical transmission analysis was performed using a spectrophotometer (JASCO-V 670), and the photoluminescence (PL) spectra were recorded using a spectrofluorometer (JASCO FP-8200). Impedance spectroscopy analysis of the PbS thin films was conducted using a CH608E instrument.

3. Results and discussion

Fig. 1 shows the X-ray diffraction (XRD) spectra of the pristine and gamma-exposed PbS films deposited on glass substrates. All the samples were found to be crystalline with the (111), (200), (221), and (311) Bragg's reflections conforming to the cubic phase of PbS [JCPDS 05–0592]. The peak intensity values increased considerably with an increase in the gamma dose. This demonstrates, that the crystallinity of the PbS thin films increases with the gamma dose. The crystallite sizes of the pristine and gamma-exposed thin films were calculated using the Scherrer equation for the main peak (111). The crystallite sizes of the pristine and gamma-exposed thin films (gamma doses of 25, 50, and 70 kGy) were 64, 83, 74, and 68 nm, respectively. The crystallites agglomerated after the gamma irradiation and lead to the formation of large crystallites. The results were in good agreement with the reported gamma irradiation thin films (Nair et al., 1993; Ali et al., 2020).

The morphology and nanostructure of the pristine and gamma-exposed PbS thin films were characterized using field-emission scanning electron microscopy (FESEM), as shown in Fig. 2 (a–d). The pristine PbS thin film exhibited a porous nature and had a granular shaped morphology with an approximately 58 nm grain size, as shown in Fig. 2 (a). Under a gamma exposure dose of 25 kGy, the granular shaped grains agglomerated together to form a cluster (Fig. 2 (b)). For values up to 25 kGy the average PbS grain size increased and then decreased with further increase in the gamma dose. The change in the morphology under the 50 and 75 kGy gamma doses were associated with the huge quantity of energy transferred to the structure in a small time interval. This is related to a change in the kinetic energy that, produced a heating effect on the surface of the PbS thin films and may have caused a change in the surface morphology and nanostructure of the PbS thin films exposed to a high gamma dose (Abhirami et al., 2013a,b).

The EDS spectra of the as prepared PbS film is shown in Fig. 2 (e) and the proportion of Pb and S are presented in the Table inset in Fig. 2 (e), which shows the good quality and purity of the PbS thin films.

Fig. 3 (a) shows the change in the optical transmission (675–1200 nm range) of the pristine and gamma-irradiated PbS thin films. The transparency in 760–1200 nm domain decreased quickly after the gamma exposure for all doses. The presence of interference fringes in the 825–1200 nm domain of the transmission spectrum shows the uniformity of thickness and homogeneity of the thin layers (Yaghmour, 2009).

The absorption coefficients (α) of the pristine and gamma exposed PbS thin films were calculated using Eq. (1).

$$\alpha = \left(\frac{1}{t}\right)\ln\left(\frac{1}{T}\right) \quad (1)$$

where t is the thickness of the PbS thin film, and T is the transmittance.

The thickness was estimated using the equation $t = \frac{M}{\rho A}$, where M is the mass of PbS deposited in grams, A is the deposited area of the thin film in cm^2, and ρ is the density of PbS (7.6 g/cm^3). The measured thickness of the deposited PbS thin film was 186 nm.

The energy band gaps of the pristine and gamma exposed PbS thin films were calculated using the Tauc equation (Eq (2)).

$$(\alpha h\nu) = A(h\nu - E_g)^m \quad (2)$$

where A is a constant, α (cm^{-1}) is the absorption coefficient, m assumes precise values ($m = 2$) depending on the type of transition, $h\nu$ (eV) is the energy of the incident photon, and E_g (eV) is the energy band gap. The energy band gaps of the PbS thin films were determined using the straight-line x-intercept of the $(\alpha h\nu)^{1/2}$ vs $h\nu$ (eV) plot shown in Fig. 3 (b).

The energy band gap decreased with an increase in the gamma dose up to 50 kGy, and then starts to increase. The energy band gaps of all

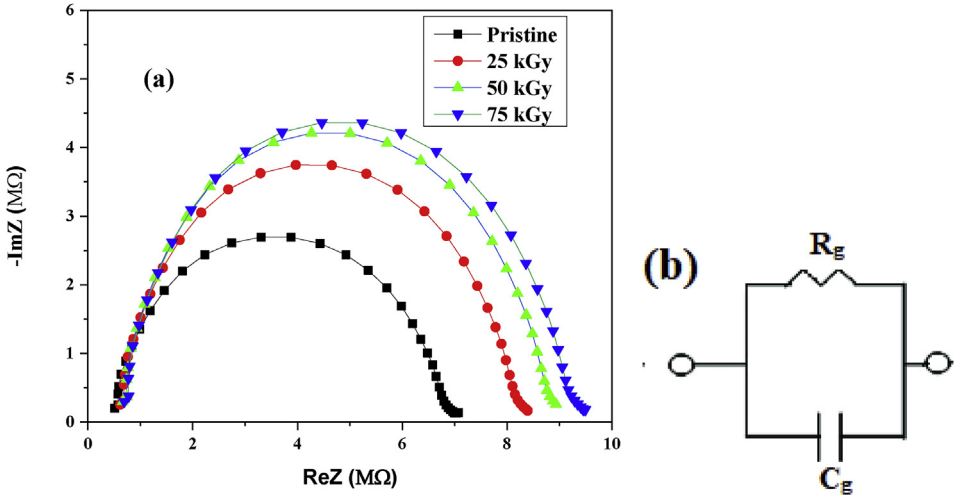

Fig. 5. (a) Nyquist plots of pristine and gamma-irradiated PbS thin films, and (b) equivalent circuit used to interpret the impedance spectroscopy data.

Table 1
Electrical parameters eliminated using impedance spectroscopy.

Sample	R_g (MΩ)	C_g (pF)
Pristine	69.4	1.38
25 kGy	82.6	1.36
50 kGy	89.3	1.36
75 kGy	93.1	1.37

the irradiated samples are less than that of the pristine PbS thin film. The reduction in the energy band gap is due to the induced defects resulting from the gamma exposure that created localized traps in the band gap (Belgacem and Bennaceur, 1990). The decrease in the band gap after the interaction of gamma rays with the PbS material is related to energy transfer, which may have caused a transfer of holes from the valence band to conduction band with an enhancement in the free electrons and holes, thereby improving the electrical conductivity of the PbS thin films (Abhirami et al., 2013a,b).

The effects of different doses of gamma exposure on the creation and eradication of defects are depicted in Fig. 4. A well-defined PL peak at 771 nm was exhibited by the pristine and gamma-irradiated PbS thin films due to the band edge transitions. Two additional peaks at 805.54 and 833.89 nm associated with the structural defects were observed in the pristine PbS thin film that was annihilated after the gamma exposure. A change in the PL peak position and intensity was observed after the gamma exposure. As the exposure dose increased, the corresponding peak intensity decreased, resulting in the position being slightly red-shifted. The slight deviation in the PL peak wavelength for the pristine and gamma-exposed PbS thin films was probably due to the structural mismatching of PbS. The decrease in the peak intensity along with the formation of a hump was due to the decrease in sulfur vacancies after the gamma exposure, and a change towards low energy (Vigil et al., 1997).

Impedance spectroscopy is a suitable technique to investigate the various gamma dose induced effects. In this study, to observe the irradiation response of PbS thin films, impedance spectroscopy was conducted before and after the irradiation at room temperature, and the results are illustrated in Fig. 5 (a) in the form of Nyquist plots. The single semicircle indicates the frequency-dependent charge transfer process, and the radius of the semicircle is associated with the charge transfer resistance. Fig. 5 (b) shows an equivalent circuit having an R–C parallel circuit, R_gC_g, associated with the charge transportation in grain boundaries. Using the selected fitting equivalent circuit model, the suitable values of the various parameters as a function of the gamma dose were determined and tabulated in Table 1. The capacitance C_g was found to be approximately the same for the pristine and gamma-irradiated PbS thin films. However, the value of the resistance R_g increased with an increase in the dose level of gamma exposure. This may have been owing to an increase in the grain size with the gamma exposure dose.

4. Conclusions

In this study, the PbS thin films were deposited on glass substrates using the SILAR technique and the structural, optical, morphological, and electrical characteristics were investigated successfully by XRD, FESEM, EDS, UV–Vis, photoluminescence, and impedance spectroscopy analysis before and after irradiation with different gamma doses. The XRD results indicated nanocrystalline thin films with (111), (200), (221), and (311) Bragg's reflections, conforming to the cubic phase of PbS thin films. The crystallinity of the thin films increased with the gamma dose. FESEM revealed that the change in morphology at 50 and 75 kGy gamma doses was associated with the large amount of energy transferred to the structure; this produced a heating effect on the surface of the PbS thin films. The reduction in the energy band gap was due to the defects induced by gamma exposure, which created localized traps in the band gap. The PL peak position and intensity changed after gamma irradiation because of a lattice mismatch of the structure. Impedance spectroscopy revealed that the grain capacitance was approximately the same for the pristine and gamma-exposed PbS thin films. However, the grain resistance increased with the gamma exposure dose. Gamma irradiation dose dependent variations were accountable for altering the properties of the PbS thin films that, can be used for radiation sensing application.

CRediT authorship contribution statement

Syed Mansoor Ali: Conceptualization, Writing - original draft, Investigation, Methodology, Supervision. **M.S. AlGarawi:** Writing - review & editing. **S. Aldawood:** Formal analysis, Funding acquisition, Project administration, Resources, Software, Validation, Visualization, Data curation. **S.A. Al Salman:** Writing - review & editing. **S.S. AlGamdi:** Writing - review & editing.

Declaration of competing interest

Authors declared that don't have any conflict of interest.

Acknowledgements

The authors would like to extend their sincere appreciation to the Deanship of Scientific Research at King Saud University for funding under Research Group No. RG-1441-315.

Appendix A. Supplementary data

Supplementary data to this article can be found online at https://doi.org/10.1016/j.radphyschem.2020.108732.

References

Abhirami, K., Matheswaran, P., Gokul, B., Sathyamoorthy, R., Kanjilal, D., Asokan, K., 2013a. Effect of SHI irradiation on the morphology of SnO2 thin film prepared by reactive thermal evaporation. Vacuum 90, 39. https://doi.org/10.1016/j.vacuum.2012.09.013.

Abhirami, K., Sathyamoorthy, R., Asokan, K., 2013b. Structural, optical and electrical properties of gamma irradiated SnO thin films. Radiat. Phys. Chem. 91, 35–39. https://doi.org/10.1016/j.radphyschem.2013.05.030.

Ali, S.M., AlGarawi, M.S., Farooq, W.A., Atif, M., Hanif, A., AlMutairi, M.A., Shar, M.A., 2020. Gamma dose dependent structural, optical and current-voltage characteristics of CdS/p-Si heterojunction. Mater. Chem. Phys. 240, 122243. https://doi.org/10.1016/j.matchemphys.2019.122243.

A-Sofiany, S.M., Hassan, H.E., Ashour, A.H., Abd El-Raheem, M.M., 2014. Study of gamma-rays enhanced changes of the ZnO:Al thin film structure and optical properties. Int. J. Electrochem. Sci. 9, 3209. http://creativecommons.org/licenses/by/4.0.

Atanassova, E., Paskaleva, A., Konakova, R., Spassov, D., Mitin, V.F., 2001. Influence of γ radiation on thin Ta2O5–Si structures. Microelectron. J. 32, 553–562. https://doi.org/10.1016/S0026-2692(01)00043-X.

Azmy, N., Azwen, N., Bakar, A., Ashrif, A., Norhana, A., Sarada, I., 2017. Enhancement of ZnO-rGO nanocomposite thin films by gamma radiation for E. coli sensor. J. Appl. Surf. Sci. 392, 1134. https://doi.org/10.1016/j.apsusc.2016.09.144.

Ballard, S.S., Browder, J.S., Ebersole, J.F., 1972. American Institute of Physics Handbook, third ed. D.E. Gray McGraw-Hill Book Co., N.Y.

Bickulova, N.N., Biskulova, V.T., Yugafarva, Z.A., 1995. 10th Int. Conf. Solid State Ionics, ABSV SSI-10. North Holland Pub., Singapore.

Belgacem, S., Bennaceur, R., 1990. Propriétés optiques des couches minces de SnO_2 et $CuInS_2$ airless spray. J. Phys. Arch. 25, 1245–1258. https://doi.org/10.1051/rphysap:01990000250120124500.

Chatterjee, A.P., Mitra, P., Mukhopadhyay, A.K., 1999. Chemically deposited zinc oxide thin film gas sensor. J. Mater. Sci. 34, 4225. https://doi.org/10.1023/A:1004694501646.

Chen, W.S., Stewark, J.M., Mickelson, R.A., 1985. Polycrystalline thin-film $Cu_{2-x}Se$/CdS solar cell. Appl. Phys. Lett. 46, 1095. https://doi.org/10.1063/1.95773.

Chopra, K.L., Major, S., Panday, D.K., 1983. Transparent conductors—a status review. Sol. Cell. 1, 102. https://doi.org/10.1016/0040-6090(83)90256-0.

Danko, V.A., Indutnyi, I.Z., Kudveryavslav, A.A., Minko, V.I., 1991. Photodoping in the As_2S_3Ag thin-film structure. Phys. Status Solidi 124, 235. https://doi.org/10.1002/pssa.2211240122.

Hirata, H., Higashiyama, K., 1971. Analytical study of the lead ion-selective ceramic membrane electrode. Bull. Chem. Soc. Jpn. 44, 2420. https://doi.org/10.1246/bcsj.44.2420.

Hsu, C., Chen, C., Chen, D., 2013. Decoration of PbS nanoparticles on Al-doped ZnO nanorod array thin film with hydrogen treatment as a photoelectrode for solar water splitting. J. Alloys Compd. 554, 45–50. https://doi.org/10.1016/j.jallcom.2012.11.192.

Ivanov, L.I., Platov, Y.M., 2004. Cambridge. International Science Publishing, UK.

Joshi, R.K., Kanjilal, A., Sehgal, H.K., 2004. Solution grown PbS nanoparticle films. Appl. Surf. Sci. 221, 43. https://doi.org/10.1016/S0169-4332(03)00955-3.

Kanazawa, H., Adachi, S., 1998. Optical properties of PbS. J. Appl. Phys. 83, 5997. https://doi.org/10.1063/1.367466.

Kane, R.S., Cohen, R.E., Silbey, R., 1996. Theoretical study of the electronic structure of PbS nanoclusters. J. Phys. Chem. 100, 7928. https://doi.org/10.1021/jp952869n.

Maheswassharon, K.S., Ramaiah, M.K., Neumann, M.S., Levy-Clement, C., 1997. Electrodeposition of lead sulfide in acidic medium. J. Electroanal. Chem. 436, 49–52. https://doi.org/10.1016/S0022-0728(97)00124-1.

Mehdi, S., Nefzi, C., Zeineb, S., Arbi, M., Ruxandra, V., Najoua, K.T., 2018. Improved structural properties, morphological and optical behaviors of sprayed Cu_2ZnSnS_4 thin films induced by high gamma radiations for solar cells. Mater. Sci. Semicond. Process. 83, 50–57. https://doi.org/10.1016/j.mssp.2018.04.009.

Meldrum, F.C., Flath, J., Knoll, W., 1996. Formation of patterned PbS and ZnS films on self-assembled monolayers. Langmuir 13, 2033. https://doi.org/10.1016/S0040-6090(99)00044-9.

Nair, M.T.S., Nair, P.K., Zingaro, R.A., Meyers, E.A., 1993. Enhancement of photosensitivity in chemically deposited CdSe thin films by air annealing. J. Appl. Phys. 74 (3), 1879. https://doi.org/10.1063/1.354796.

Nair, P.K., Gomezdaza, O., Nair, M.T.S., 1992. Metal sulphide thin film photography with lead sulphide thin films. Adv. Mater. Optic. Electron. 1, 139. https://doi.org/10.1002/amo.860010307.

Nefzi, C., Souli, M., Beji, N., Mejri, A., Kamoun-Turki, N., 2017. Enhancement by high gamma radiations of optical and electrical properties of indium oxide thin films for solar devices. J. Mater. Sci. 52 (1), 336–345. https://doi.org/10.1007/s10853-016-0334-5.

Obaid, A., Mahdi, M., Hassan, Z., 2012. Growth of nanocrystalline PbS thin films by solid-vapor deposition. Adv. Mater. Res. 620, 1–6. https://doi.org/10.4028/www.scientific.net/AMR.620.1.

Patel, J., Mighri, F., Ajji, A., Tiwari, D., Chaudhuri, K., 2014. Spin-coating deposition of PbS and CdS thin films for solar cell application. Appl. Phys. A 117, 1791–1799. https://doi.org/10.1007/s00339-014-8659-x.

Putley, E.H., 1967. Materials Used in Semiconductor Devices, second ed. John Wiley and Sons Ltd., N.Y.

Seghaier, S., Kamoun, N., Brini, R., Amara, A., 2006. Structural and optical properties of PbS thin films deposited by chemical bath deposition. Mater. Chem. Phys. 97, 71–80. https://doi.org/10.1016/j.matchemphys.2005.07.061.

Shabir, A., Asokan, K., Khan, M.S., Zulfequar, M., 2015. Structural and optical analysis of 60Co gamma-irradiated thin films of polycrystalline $Ga_{10}Se_{85}Sn_5$. J. Radiat. Eff. Defect Solid 170, 956. https://doi.org/10.1080/10420150.2016.1141906.

Thangaraju, B., Kalainnan, P., 2000. Preparation of nanocrystalline Cd-doped PbS thin films and their structural and optical properties. Sci. Technol. 15, 849–853. https://doi.org/10.1016/j.jtusci.2017.05.001.

Torimoto, T., Takabayashi, S., Mori, H., Kuwabata, S., 2002. Photoelectrochemical activities of ultrathin lead sulfide films prepared by electrochemical atomic layer epitaxy. J. Electroanal. Chem. 522, 33. https://doi.org/10.1016/S0022-0728(01)00753-7.

Vigil, O., Riech, I., Garcia, M.R., Zelaya, O.J.A., 1997. Characterization of defect levels in chemically deposited CdS films in the cubic-to-hexagonal phase transition. J. Vac. Sci. Technol., A 15, 2282. https://doi.org/10.1116/1.580735.

Yaghmour, S.J., 2009. Influence of γ-irradiation on optical properties of manganese phthalocyanine thin films. J. Alloys Compd. 486, 284–287. https://doi.org/10.1016/j.jallcom.2009.06.135.

Yonghong, N., Wang, F., Hongfiang, L., Yin, G., Hong, J., Ma, X., Xu, Z., 2004. A novel aqueous-phase route to prepare flower-shaped PbS micron crystals. J. Cryst. Growth 262, 399–402. https://doi.org/10.1016/j.jcrysgro.2003.10.053.

Zhu, R.Y., 1998. Radiation damage in scintillating crystals. Nucl. Instrum. Methods Phys. Res. 413, 297–311. https://doi.org/10.1016/S0168-9002(98)00498-7.